RSC Advances

PAPER

View Article Online
View Journal | View Issue



Cite this: *RSC Adv.*, 2022, **12**, 31215

# Instant *in situ* formation of a polymer film at the water–oil interface†

Sara Coppola, *[a] Lisa Miccio,[a] Zhe Wang,[b] Giuseppe Nasti,[a] Vincenzo Ferraro,[b] Pier Luca Maffettone,[b] Veronica Vespini,[a] Rachele Castaldo,[c] Gennaro Gentile[c] and Pietro Ferraro[a]

The water–oil interface is an environment that is often found in many contexts of the natural sciences and technological arenas. This interface has always been considered a special environment as it is rich in different phenomena, thus stimulating numerous studies aimed at understanding the abundance of physico-chemical problems that occur there. The intense research activity and the intriguing results that emerged from these investigations have inspired scientists to consider the water–oil interface even as a suitable setting for bottom-up nanofabrication processes, such as molecular self-assembly, or fabrication of nanofilms or nano-devices. On the other hand, biphasic liquid separation is a key enabling technology in many applications, including water treatment for environmental problems. Here we show for the first time an instant nanofabrication strategy of a thin film of biopolymer at the water–oil interface. The polymer film is fabricated *in situ*, simply by injecting a drop of polymer solution at the interface. Furthermore, we demonstrate that with an appropriate multiple drop delivery it is also possible to quickly produce a large area film (up to 150 $cm^2$). The film inherently separates the two liquids, thus forming a separation layer between them and remains stable at the interface for a long time. Furthermore, we demonstrate the fabrication with different oils, thus suggesting potential exploitation in different fields (*e.g.* food, pollution, biotechnology). We believe that the new strategy fabrication could inspire different uses and promote applications among the many scenarios already explored or to be studied in the future at this special interface environment.

Received 12th July 2022
Accepted 18th October 2022

DOI: 10.1039/d2ra04300a

rsc.li/rsc-advances



## Introduction

Over the last decade, a wide range of functional materials and protocols have been investigated for controlling the formation of monolayers at the interface between two immiscible materials (liquid/liquid interface).[1] Various technological strategies proposed solutions focused on the formation of surfactant monolayers of different chemical nature (*e.g.* proteins, lipids) as well as on the self-assembling at the interface of solid particles from nano to microscale.[2–4] The knowledge of this phenomena is crucial for various areas as diverse as life science, food packaging, environmental sciences, electronic and more in general technology. Particles at the interfaces between two liquids have been used to study aggregate morphologies in terms of flocculation, phase separation, and self-assembly.[5] The results have been used for the conformational stability of proteins in food emulsion, which has important implications for improving emulsion properties under thermal processing in industry[6] as well as for controlling the microbial contamination of stored diesel/biodiesel fuel over time and the consequent changes in the fuel chemical composition.[7] More in general, the strategy of oil–water self-assembly has become one of the most intriguing fields in nanoscience and nanotechnology due to the unique properties and important applications of these functional films in nanodevices and electronics.[8,9] Although the proposed strategies demonstrate many advantages, some deficiencies also exist and the use of multiple, different and active materials still call nowadays for flexible methods for film fabrication, which might possibly guarantee self-adaptation even to complex geometries.

More in general, in the last several decades, different studies have investigated for thin-film fabrication such as methods including interfacial polymerization, stretching, track-etching and electrospinning.[10,11] Spin-coating,[12,13] casting,[14] and Langmuir–Blodgett methods[15,16] have been mainly used for the fabrication of membranes but, the very thin films obtained by these methods are difficult to handle. Many different techniques exist for the handling methods and peeling off protocols

[a]*CNR-ISASI, Institute of Applied Sciences and Intelligent Systems "E. Caianiello", Via Campi Flegrei 34, 80078 Pozzuoli, Napoli, Italy. E-mail: sara.coppola@cnr.it*
[b]*Dipartimento di Ingegneria Chimica dei Materiali e della Produzione Industriale, Università degli Studi di Napoli "Federico II", Piazzale Tecchio 80, 80125 Napoli, Italy*
[c]*Institute for Polymers, Composites and Biomaterials, CNR, Via Campi Flegrei 34, 80078 Pozzuoli, Italy*

† Electronic supplementary information (ESI) available: Movies S1 and S2. See DOI: https://doi.org/10.1039/d2ra04300a

for very thin membranes.[12] However, even if these methods offers solution for direct handling of very thin films, they reduce at the same time the flexibility of the fabrication method and the real case of use. Moreover, in case of casting, membrane uniformity can be achieved only with manual manipulation. The increased demand for effective polymeric membrane fabrication techniques opened also towards new manufacturing technologies, among the additive manufacturing techniques, fused deposition modelling, stereolithography and selective laser sintering are suitable for polymer processing to this end.[17–21] Unfortunately, such process is still based on a multi-step approach, very expensive devices are involved and the thin-film formation *in situ*, especially in commercial device, remains a challenge.[22] Among the most common techniques to form membranes from liquid films made of polymer solutions there are thermally induced phase separation (TIPS), dry-casting induced by vapor/evaporation phase inversion separation (VIPS) and wet-casting based on non-solvent phase separation (NIPS).[23–26] Furthermore, there are partially empirical models and simulations that can predict their evolution with good approximation. These models are based on the conservation of mass, energy and momentum. The most valuable tools used to understand the evolution of these systems are the so-called "composition" or "mass-transfer" paths, which are time-dependent concentration profiles plotted directly on phase diagrams of the polymeric/solvent/nonsolvent systems and are used to predict the time required for phase separation to occur from immersion and the concentration profile within the film during the demixing process. However, until now, most of the studies have been aimed at the formation of thin-films on rigid substrates[27,28] while the formation of suspended and easily adaptable thin films is still a challenge.

In the present research we deal about formation of floating thin-films on liquids based on previous work. In fact, very recently we proposed a water-based bottom-up approach for the straightforward shaping of polymeric membranes and the encapsulation of microbodies on arbitrary substrates. The process guided the self-assembly of a biocompatible polymer over the water surface. Being a liquid, water can take flexible forms, and as a direct result, the self-assembled encapsulation membrane could wrap in different geometries, generating a thin polymeric film following the existing water profile and eventually sealing all the elements included in it.[29]

Here we propose a completely new method for easy and quick formation of thin polymer film at the special setting of stratified oil/water interface. This technique is a very fast method for the creation of a polymeric thin-film in the two liquids environment. Starting from previous results achieved at air/water surface, we show here that the process can be equally adapted to make a thin polymeric layer between two liquids. Such method extends the application of this technique thus enlarging exploitation to many cases of use where water/oil liquids are involved. We tested different kind of oils, used for different application: food, biology, and engines. The biofilms are formed *in situ*, directly in the place of interest without the need of handling and the consequent risk of deforming and damaging them. We demonstrate by different experiments that the thin polymeric film can float at interface, *i.e.*, it remains where it forms, for prolonged time. The *in situ* formation could be realized in a single shot or by appropriate multiple dispensing. Guided by self-assembling, the polymer film could form even in complex geometries and in small as well as macro scale. In fact, the shape of the container used for the liquid and its boundary will guide the polymeric spreading. The self-assembling guided procedure also allowed to create thin-films of desired dimension and shape. In this way it is possible to use biocompatible materials avoiding the direct contact, the preformation by stamps and the need to cut prefabricated big membrane. The membrane could be harvested from the liquid and used for coatings. A first exploitation of thin film formed in a macro scale device is here proposed like case of use. The produced thin-films are thoroughly characterized with SEM microscopy and holographic interferometry. The results reported here make available a novel fabrication method that could be exploited at oil/water interface thus opening new possibilities for applications of nanotechnology located at this special and rich setting-realm between such two liquids.

## Materials

PLGA Resomer RG 504H (38 000–54 000 Da; 50 : 50 lactide : glycolide, Boerhinger Ingelheim) was dissolved in DMC (99%; Sigma-Aldrich) at 25 w%. For the experiment of sealing the syringe the PLGA ink was doped with a fluorochrome (Nile red, $C_{20}H_{18}N_2O_2$, technical grade, Sigma-Aldrich, 2 μg per milligram of PLGA. Mineral oil (Sigma-Aldrich) was used as received. Diesel Engine oil (Q8) and olive oil (Carapelli oil) were used as received without further purification. Density of mineral oil MOil $\sim$ 0.80–0.88 g cm$^3$; density of diesel oil DOil $\sim$ 0.82–0.85 g cm$^{-3}$); density of olive oil EVOil $\sim$ 0.92 g cm$^{-3}$.

### Preparation of bio-films at the water/oil interface

Biofilms were prepared at the interface between water and oil. We prepared a polymeric solution of poly lactic-*co*-glycolic acid (PLGA) dissolved in dimethyl carbonate (DMC) with a concentration of 25% PLGA in DMC w/w. Untreated tap water was poured in a glass beaker and covered with a thick layer of oil, forming two different phases (stratified oil/water mixture) with oil on top of water due to its lower density (Fig. 1a). The oil was dispensed using a syringe and controlling the rate of dispensing to prevent the formation of submerged oil drops in the water phase. The beaker was left still for few minutes to reach a static condition of the fluids. We used three different oils to prove the process of biofilm formation in different conditions: mineral oil (MOil), diesel fuel (DOil) and extra-virgin olive oil (EVOil). A 2 μl drop of the DMC/PLGA solution, was then carefully released at the interface between the two liquids as depicted in Fig. 1. The needle was located at $\sim$1 mm height from the interface for all the experiments to ensure that the starting conditions of the spreading were the same for all the experiments. The higher density of the polymer solution, compared to the oil phase, guaranteed the sedimentation of the drop towards the oil/water interface.

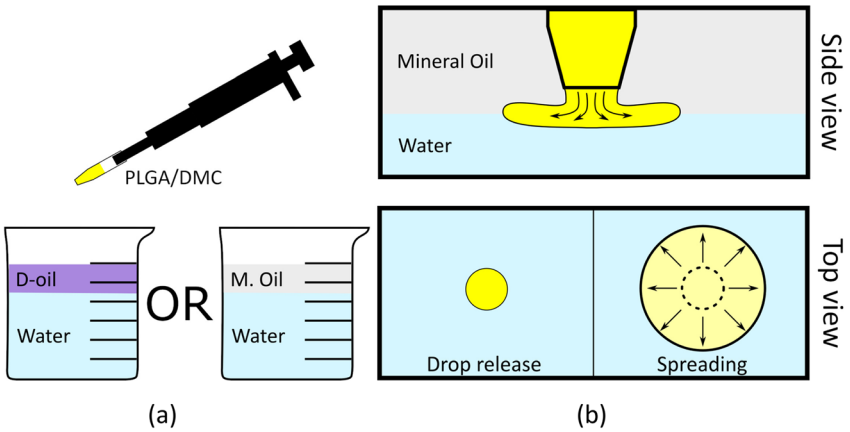


Fig. 1 Schematic representation of the biofilm formation: (a) the glass beaker is filled up with tap water and then covered with MOil or DOil. A small amount of PLGA/DMC (yellow in the figure) solution is released in the proximity of the oil/water interface. (b) Once the tip of the pipette is submerged in the oil layer, the solution is dispensed at the interface oil/water. The PLGA/DMC solution, due to the Marangoni effect and to the extraction of DMC in water, spreads at the oil/water interface and forms a thin solid film between the two phases.

Two phenomena occur upon insertion of the polymer solution drop between the water and oil phases: drop spreading thus forming a thin film, and diffusion of DMC from the drop to the water.

Spreading of the deposited drop is expected given the interfacial tensions of the system. The spreading coefficient S is defined as:

$$S = \sigma_{12} - (\sigma_{13} + \sigma_{23}) \quad (1)$$

where $\sigma_{12}$ is the interfacial tension between water and oil, $\sigma_{23}$ between oil phase and the PLGA solution, $\sigma_{13}$ the one between water and the PLGA solution. The value of the last term can be considered zero because DMC is soluble in water (as also PLGA). As $\sigma_{23} < \sigma_{12}$ then $S$ is positive and spreading of the PLGA in DMC drop is expected. On a slower timescale, DMC diffuses in the water leading to polymer solidification and the formation of the polymer film.

This process ends in the formation of a circular thin-film between the two phases (Fig. 1b). The shape of the as formed film usually presented a round shape while the surface area clearly depended on the volume of solution dispensed at the interface (see ESI Movie S1†). This interface acted as a barrier for the fluid because of interfacial energy and insolubility of PLGA in water.

The self-standing thin-film is shown in Fig. 2a. Because of its transparency, typical of the PLGA used in the experiment, the presence of the film could be revealed only from a side view observation (Fig. 2b), or, alternatively, by moving the beaker and looking to the film oscillating at the interface. The film could be easily manipulated and recovered from the solution using a commercial microscope glass slide (Fig. 2c) as explained in the following.

Once formed and solidified, the film started to dry and a significant modification of its appearance occurred. Gradually, after few minutes, the film contrast in the liquid increased becoming white probably for the loss in homogeneity and the corresponding light scattering. In order to study this phenomenon, the thin-films were carefully recovered from below and from above using the supporting slide (Fig. 2c). The obtained

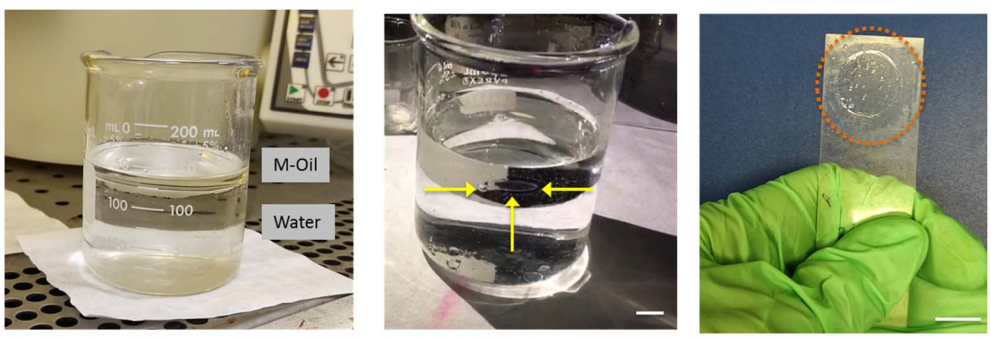


Fig. 2 (a) The glass beaker is filled up with tap water (bottom) and with MOil (up). (b) The resulting PLGA biofilm, floating at the interface is indicated by three yellow arrows; since it is transparent is can better visualized from the side view. (c) Extracted film can be released on a glass slide. For collecting the floating film the slide was submerged into the beaker. Scale bars: 1 cm.

films could be easily handled with tweezers without damaging them, while the residual oil droplets adhering to the polymer were removed by a series of ethanol washing cycles. The thin-film was visualized from a side view (Fig. 3a) and collected on the supporting target (Fig. 3b). The manipulation and recovering of the film perturbs the oil–water interface, inducing a partial mixing of the two phases. Nevertheless, after the film removal, the oil–water interface is quickly restored and it can be used to prepare new films. Thin-films formed with the three different oils appeared very similar, in terms of dimension and shape (see ESI section†). The experiment of film's formation was repeated 10 times using the same volume of water and polymeric solution, and the results were highly reproducible.

By dispensing multiple drops at oil–water interface in different locations, it was possible to produce larger film by exploiting the coalescence. In fact, the polymer solution droplets spread over the water–oil interface and coalesce, up to adhering to the glass walls of the container, thus remaining anchored and completely separating the pre-existing two phases (see Fig. 4b). The driving force of this effect is the tendency of the polymer solution to quickly spread over the water–oil interface. When two advancing circular film frontiers, emerging from two different drops of polymer solutions, meet they can mix together and, getting in touch with each other, the polymer solution coalesces, forming a single continuous thin film when DMC diffuses into the water phase. In fact, during the spreading of the solution, the edges of the membranes join together forming a single continuous larger one (Fig. 4a). By carefully and quickly dispensing the DMC/PLGA drops, the polymer film could even completely seal the oil/water interface. Such a large big film could even adhere to the glass wall of the container thus remaining anchored and completely separating the pre-existing two phases as shown in Fig. 4b. After the coalescence, once the membrane was anchored to the glass, and because of its transparency it is hard to detect it. In order to easily display the resulting membrane, we created some surface wrinkles by touching the polymeric film with a tip (Fig. 4b).

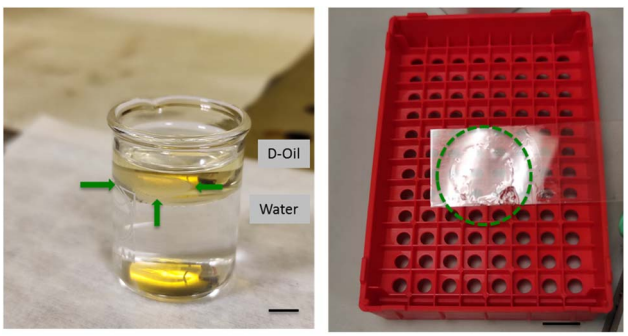


Fig. 3 (a) The glass beaker is filled up with tap water (bottom) and with DOil (up). The resulting PLGA biofilm, indicated by three green arrows; since it is transparent it better visible from the side view (scale bar 0.5 cm). (b) A commercial glass slide is used for collecting the floating film. In order to help the visualization a green dotted ring is sketched around the collected sample (scale bar 1 cm).

### Morphological analysis by SEM

The morphology of the thin-films was investigated by SEM analysis. SEM micrographs reported in Fig. 5 demonstrate that the proposed process was able to generate ultrathin membranes. As show in Fig. 5a, the film prepared at the MOil/water interface was characterized by a thickness of about 2 μm. Similar thickness values (1–2 μm) were recorded for all the films, included those prepared at the DOil/water interface. Moreover, all the obtained films had an asymmetric structure with regular top and bottom surface morphologies. The top surface (Fig. 5b) of the sample prepared at the MOil/water interface showed localized circular defects whose size is in the range 0.3–0.5 μm. A similar morphology was observed when the film surface was generated in contact with the casting diesel fuel phase (Fig. 5d). In this case, nanosized wrinkles were also evidenced. On the contrary, the samples generated in contact with the water phase were very flat and regular, with no peculiar morphological features, either for the sample generated at the mineral oil/water interface (Fig. 5c) either for the samples

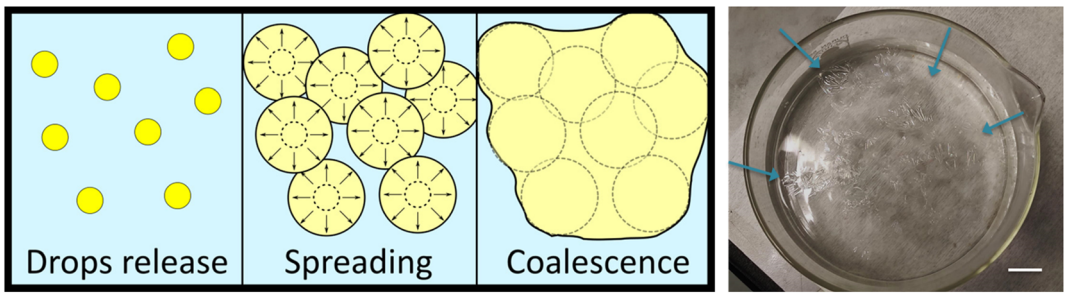


Fig. 4 (a) Schematic formation of biofilm formed by more than one dispensed drop. Multiple drops were released at the interface. During the spreading of the corresponding film one film merged spontaneously with the adjacent ones. At the end of the spreading process, a single larger film is formed. Controlling the dispensed volume, it would be possible to tune the area of the polymeric film. (b) The resulting PLGA biofilm was formed by multiple dispensing on a macroscale (radii beaker 7 cm). For the shown film the aspect ratio area/thickness is $\sim 5 \times 10^4$. Some wrinkles were formed using a tip in contact with the polymeric film to revealing the presence of the formed sample (see the blue arrows), scale bar 2 cm. Some welding lines are also visible.

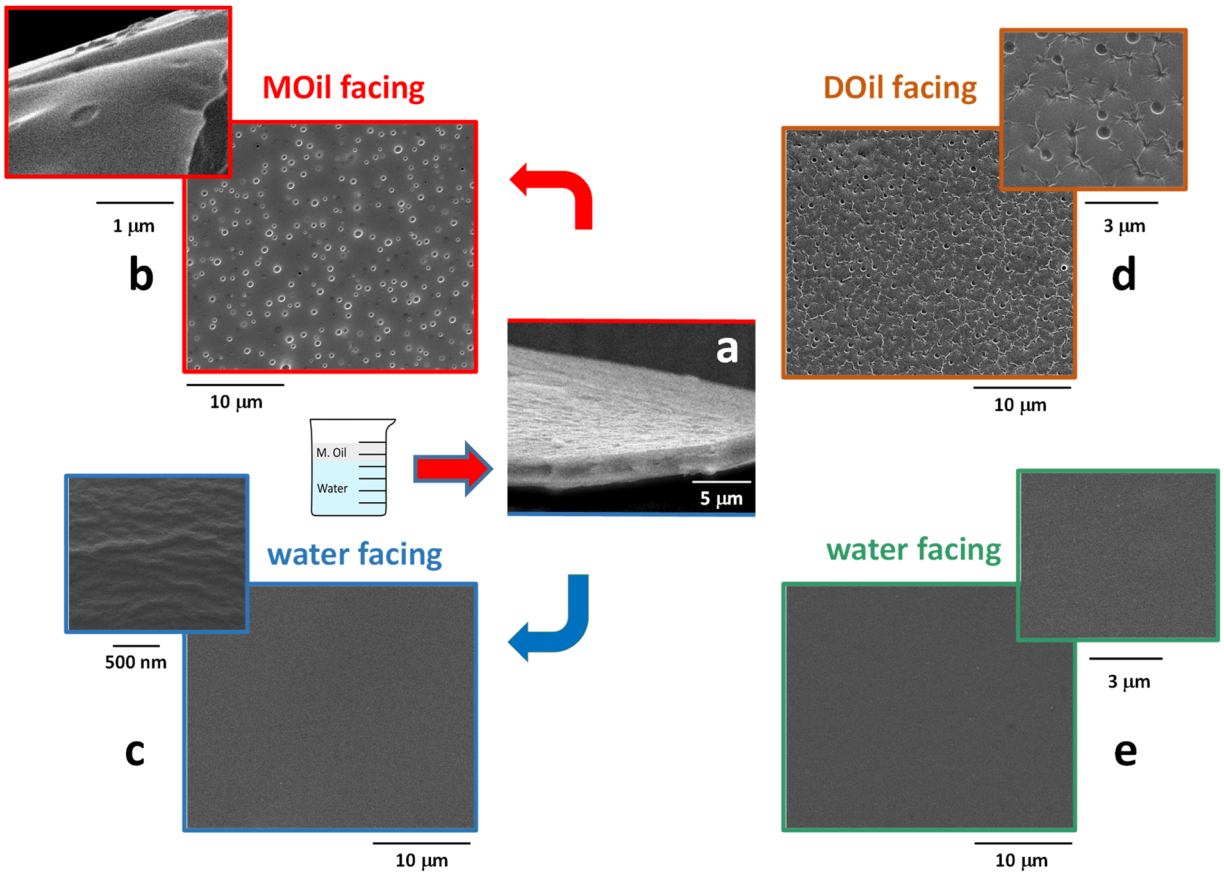


Fig. 5 SEM images of the membrane generated at the MOil/water interface (a–c) and at the DOil/water interface (d and e). (a) Side view of the membrane; (b) top view of the membrane, showing the surface generated at the interface with MOil; (c) bottom view of the membrane, showing the defects-free surface generated at the interface with water; (d) top view of the membrane, showing the surface generated at the interface with DOil; (e) bottom view of the membrane, showing the defects-free surface generated at the interface with water.

generated at DOil/water interface (Fig. 5e). Hence, the morphological analysis clearly revealed the non-porous structure of the thin-film. The sub-micrometric voids evidenced at both the oil-facing sides (MOil and DOil) do not propagate through the whole section generating a membrane porosity. Instead, they are micro-depressions characterized by a very low depth, approximately in the range of hundreds of nanometers, as shown by the high magnification SEM image in Fig. 5b. This oil facing surface morphologies are consistent with the accepted formation mechanism of surface micro voids in asymmetric thin-films, deriving from an osmotic shock between a solution and a casting medium with a relatively good mixing tendency with the polymer solution. When the interface is formed, an abrupt rupture occurs, and the micro-depression are generated through a rapid diffusion of the non-solvent oil into the polymer solution.[30] This mechanism also explains the formation of wrinkles, generated during the setting of the membrane by the difference of the viscoelastic properties between the hard skin formed on the top side of the nascent membrane, in contact with the casting DOil phase, and the viscoelastic polymer solution underneath.[31] Interestingly, these wrinkles were only present when the sample was generated at the DOil/water interface, possibly because the higher viscosity of the mineral oil phase (15–20 cSt *vs.* 2–4 cSt for DOil measured at 40 °C) induces the formation of a more regular top surface of the film, with micro-voids characterized by a lower depth and the absence of wrinkles.

On the other side, the flat, regular bottom surface, generated at polymer solution/water interface, is similar to that already evidenced in a previous work, where we reported their complete mechanical characterization.[31] In this case, the low mixing tendency of the PLGA/DMC solution and the water casting medium, combined with a tailored concentration and viscosity of the PLGA solution, allowed its fast spreading over the water surface and the quick formation of void-free PLGA skin surfaces. The film extension, its thickness and, eventually surface distribution of the holes could be controlled by varying the characteristics of the polymer solution and the two casting media, thus allowing to tailor the transport properties of the film.

### Interferometric characterization

In order to have a full-field characterization of the thin-film over large areas we employed an interferometric measuring method. We used digital holography (DH) that is one of the state-of-the-art microscopy technologies proven to be an effective tool for

revealing thickness mapping of complex and dynamic thin films[32,33] and as metrology tool at micro-nanoscale for soft matter.[34] Herein, off-axis DH geometry is used to measure the thickness in static condition after the film has been extracted from the water/oil interface (Fig. 6).

The holographic recording system is based on an off-axis Mach–Zehnder interferometer showed in Fig. 6b. Detailed description of the setup and quantitative data analysis is reported in ESI section.†

Fig. 6c–g show the holographic measurement results for static thin-film sample. The fully dried sample was spread flat on the Petri dish and placed in the object arm of the recording setup. Fig. 6c shows the digital hologram recorded by the camera, which is numerically processed by Matlab© code to retrieve amplitude imaging (Fig. 6d), and quantitative phase contrast map. Herein, the amplitude image helps to clarify the boundary of the sample, as shown by the black area at the centre on the figure. Thickness map was retrieved from quantitative phase distribution, 2D and 3D representations are showed in Fig. 6e and f respectively. For the numerical reconstruction process of digital holograms, the phase information indicates the optical path difference (OPD) between the object beam and the reference beam. In static membrane recording experiments, the samples in object arm include membrane and glass slide. The conventional single exposure method cannot accurately separate the thickness information of the membrane; therefore, two-step exposure method is used to obtain its thickness. Firstly, a background hologram which just contain the transmission information of glass slide should be recorded; after this, the target hologram needs to be acquired under the same conditions when membrane is placed. As the last step, the phase extraction of the object of interest is achieved by subtracting the reconstruction information of the background hologram from the target hologram. Once the phase $\varphi_0$ only represents the optical path difference caused by the thin membrane, the thickness information can be calculated by the following formula:

$$h_0 = \frac{\lambda \varphi_0}{2\pi n_o}$$

where $\lambda$ is wavelength of recording beam, which is 632.8 nm; $n_o$ is the refractive index of membrane, which is 1.47. In this case, the full FoV thickness mapping of membrane can be acquired statically.

Interestingly, we noticed that in the field of view (FoV) of this measurement, a sort of channelling effect has appeared at the left of the boundary, it also can be found in Fig. 6a as the red arrows indicate. This is most likely caused by the solvent diffusion process during the film forming that creates itself a sort of "leak" path. A reasonable explanation would be that during the membrane formation process, the edge thickness is higher than the membrane center thickness, and the solvent

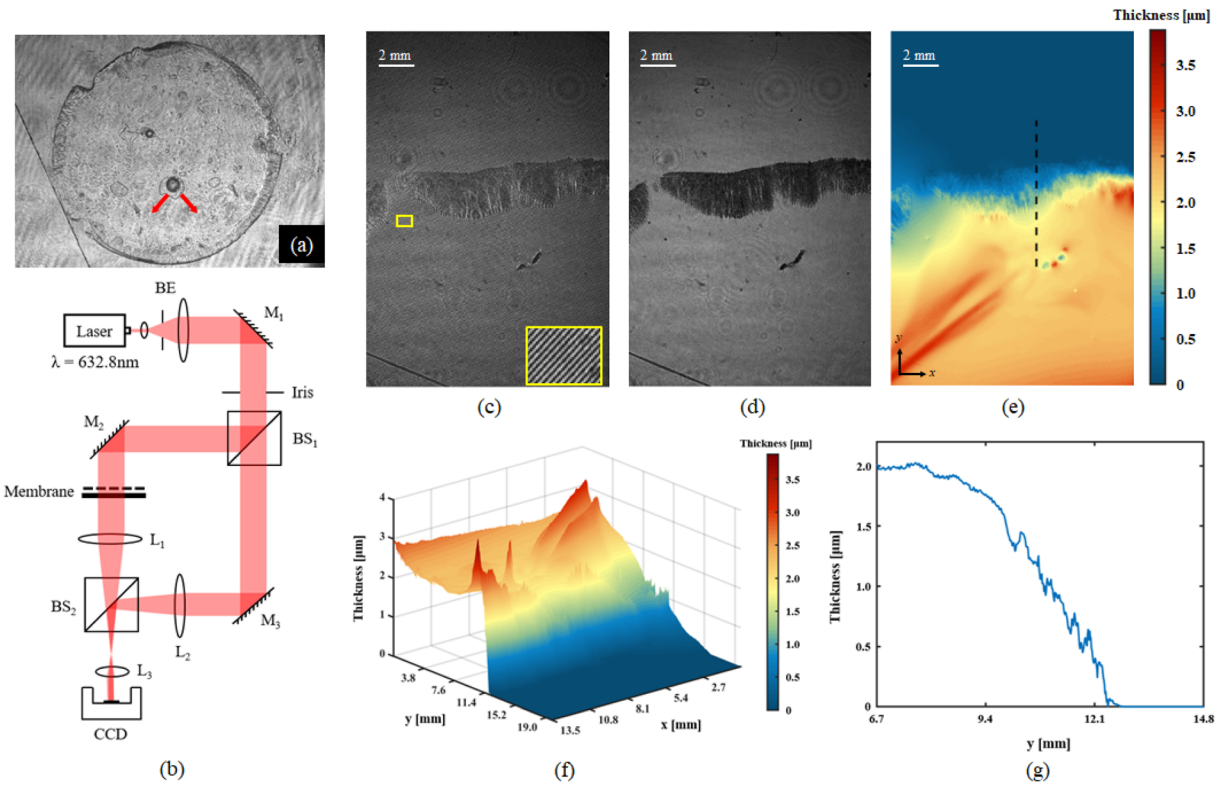


Fig. 6 (a) Transmission intensity image of the whole membrane, the red arrows indicate the 'leaks'. (b) Optical setup for interferometric measurements. (c) Digital Hologram of static membrane, placed on a clean Petri dish. (d) Holographic amplitude imaging result. (e) Two-dimensional holographic thickness mapping of recorded membrane. (f) Three-dimensional holographic thickness mapping. (g) Membrane thickness (μm) along the sectional view of dotted line in (e).

diffuses from the center to the periphery during the entire forming process and accumulates at the edge. Once the internal pressure is greater than the external pressure, a 'leak' will be formed at the edge.

After dropping a droplet at the oil and water interface, DH recording was applied in 221 s for imaging the spreading and the membrane formation process. The frame rate of recording was set to 15 FPS. A circular FoV with diameters 10.35 mm was chosen to show the selected membrane area. Herein, thanks to the phase imaging capability pf DH, no special staining process is required to observe changes in transparent membrane. The phase information is affected by both membrane and PLGA/DMC layer thicknesses, it can be regarded as a hybrid to characterize PLGA dynamic process. Fig. 7a shows the phase images of five selected time points, to reveal the representative interface distributions. The complete spreading and membrane formation is showed in the ESI Movie S3.†

Herein, the recorded full life circle three-dimensional phase information is associated with time information, a spatiotemporal model for representing the forming process of membrane is established, as shown in Fig. 7b. In the model, axis-*x* represents the time; axis-*y* represents the radius; axis-*z* represents the average phase of related arc of the corresponding radius. After dropping the droplet, the spreading process lasted for 52.34 s. The spreading process of the solution exhibits a wave-like structure, as clearly observed from the spatiotemporal model. In 221 s, 10 waves can be found; among them, the first seven waves have well-defined configuration, which occurs within 52.34 s of delivery; this also implies the time window for the spreading process. Meanwhile, in the edge part of the membrane, where radius from 6.0 mm to 7.2 mm, a thickening process can be identified; this revealed the time window for formation of the membrane. It can be seen from the model that the self-assembling and spreading processes proceed simultaneously, and both maintain an active state for 52.34 s. Another valid evidence is shown in Fig. 7c, the moving velocity of PLGA solution during spreading is revealed. Through the analysis of time-lapse holographic images, 50 feature points in the FoV were analysed using Holographic Particle Image Velocimetry (HPIV). By averaging the velocity of 50 feature points, the overall velocity curve of the spreading process is drawn. The spreading continued to accelerate until 28.5 s; then from 42.6 s, the second decay begins. This result clear shows the active time window for dynamic spreading process. Therefore, in the case of multi-droplets forming, independent droplet spreading and membrane formation have sufficient time windows to merge with each other, which allows to form a big membrane as expected.

### *In situ* fabrication of a self-adaptable biofilm

As remarked above, we demonstrated the *in situ* quick fabrication of the thin-film between the oil/water interfaces in a stratified oil/water mixture that can act as a septum and as a barrier between the two phases. We applied the multiple dispensing technique within a syringe. After the removal of the needle, we sealed the syringe on using parafilm. We also removed the plastic piston and used the syringe just as a cylindrical container where we added 3 ml of water and, above it, 2 ml of oil (Fig. 8). Without the formation of the polymeric barrier between the two phases, the two liquids were free to switch their relative

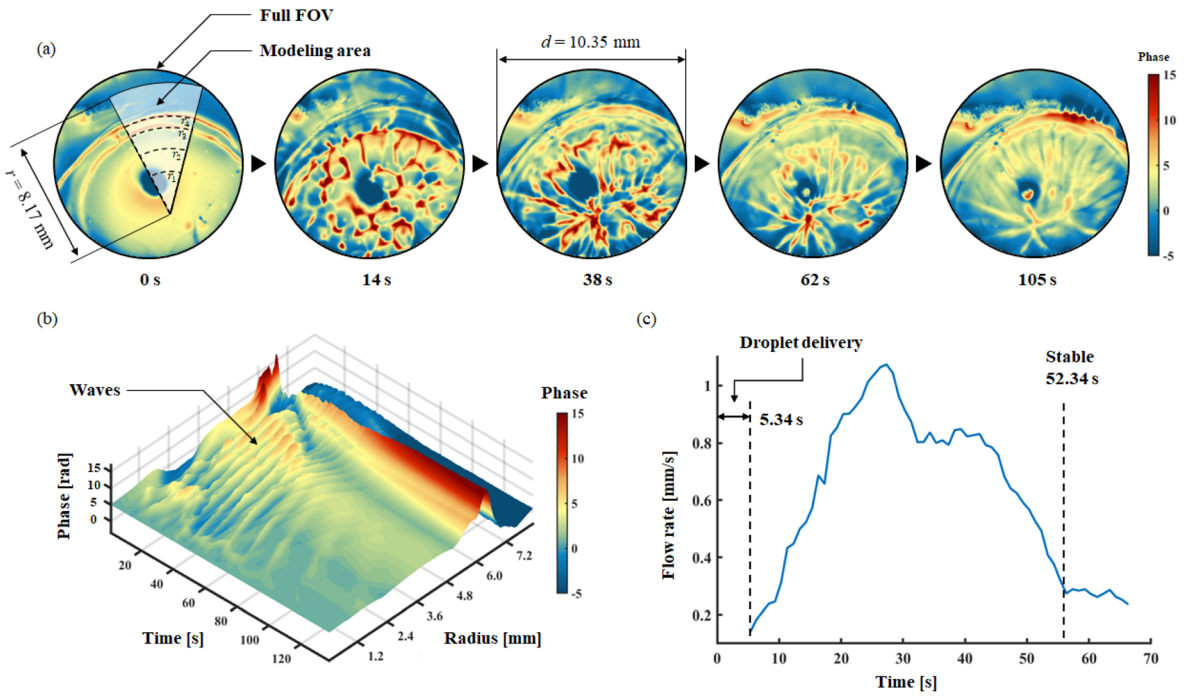


Fig. 7 (a) Five phase images of selected time points, reveal the typical forming process characteristics. (b) Space-time model of single droplet forming the membrane. (c) The curve shows the spreading speed of PLGA solution during forming process.

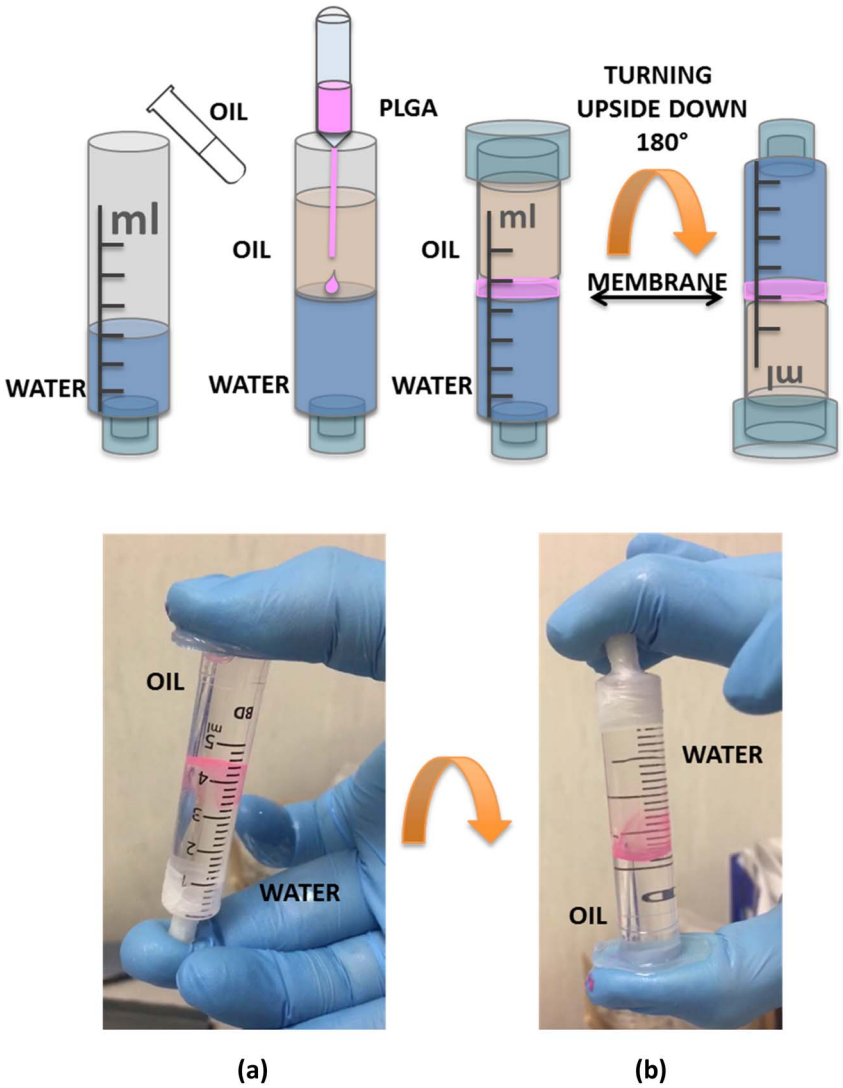


Fig. 8 Schematic representation for the *in situ* direct formation of membrane. A conventional hypodermal syringe was used as container for water and oil, after sealing its inlet with parafilm. (a) The polymeric solution, with a pink fluorophore, was dispensed at the interface. Once the membrane was formed, parafilm packaging closed the outlet. (b) Turning the syringe upside-down the two phases remained still split by the membrane.

positions, due to the different densities, whenever the syringe was rotated. We then proceeded to the *in situ* formation of the PLGA biofilm at the oil/water interface, inside the syringe, adding a pink fluorochrome (see Materials section) to improve its visibility. We filled the syringe with water and oil in the same ratio as the previous experiment and followed the same procedure. We loaded a pipette with the pink polymeric solution and inserted the needle in the oil just over the water surface, at the oil–water interface we delivered 2 μl of solution and observed the *in situ* formation of the film. As soon as the solution droplet was dispensed it was possible to observe the spreading of a circular polymeric film starting from the centre (where the solution was dispensed) toward the walls of the cylinder. The expansion stopped once the syringe walls were reached. The adhesion of the polymer to the syringe created a separating thin-film between water (bottom) and oil (top). Thanks to this polymeric septum, self-sealed all around the syringe walls, the two phases could not move freely inside the cylinder and were constrained to maintain their relative positions also after a 90° rotation of the syringe (see ESI Movie S2†).

## Conclusions

A single-step and bottom-up technology is proposed here for instant and *in situ* thin-film formation at the interface between two liquids, implemented at low working temperature (ambient temperature) and with low cost. We propose for the first time a new technology for membrane formation and its characterization in real time at the interface of two immiscible materials like in case of stratified oil/water mixture. The formation of the thin-film *in situ* has been studied showing high flexibility in the formation process. Single floating biofilms and large area coverage thin-films, obtained by multiple dispensing, have been demonstrated. The samples show an asymmetric structure with

regular and flat water-facing surface and oil-facing surface characterized by micro-voids of about 0.5 μm. The thickness of the film is about 2 μm and the thickness edge is higher than the film centre thickness. Guided by the self-spreading the polymer film formation could take place even in complex geometries where the geometry itself and its boundary will guide the polymeric spreading. Moreover, in principle, the dispensing of a polymeric solution activating the film formation, could be used in the meanwhile for the creation of a surface gradient able to induce the self-propelling of common floating objects. In this way controlling the position where the droplet is delivered and the total amount of the dispensed volume, it is possible to guide the self-assembly and tune the size, shape, and extension of the as formed film guided by the locomotion of freely floating object. Morphological SEM and quantitative full-field characterization have been reported, using digital holography. We showed that DH provides effective full-field tool for measuring the film thickness and in future it could be used for tracking the formation in real time. In fact, the process is very fast and our first results show that holography could represent a good tool for time-lapse microscopy characterization. We believe that the proposed technology could be further improved in the future also for separation of liquids, emulsified oil/water mixture, filtering and/or selective adsorption of pollutants. In fact, the polymeric membrane could be used for pollutant recovery in case of binding chemically elements on the surface after an opportune functionalization. Moreover, being the polymer used a biodegradable one we foresee application of biocompatibility. Future developments could find possible application in food science, *i.e.* for packaging and food safety, or for environmental applications for water analysis, remediation and selective adsorption of pollutants. Measurement of the spreading dynamics was outside the scope of the present research, but it will be addressed in a forthcoming work.

## Data availability

The data that support the findings of this study are available from the corresponding author upon reasonable request.

## Conflicts of interest

The authors have no conflicts to disclose.

## Acknowledgements

This work was supported by the MIUR project "Piattaforma Modulare Multi Missione" (PM3), ARS01_01181 and by the MIUR project "STRutturE intelligenti e funzionalizzAte per il Miglioramento delle prestazioni aerostrutturali" (STREAM), ARS01_01182.

## References

1 M. Mottola, B. Caruso and M. A. Perillo, Langmuir films at the oil/water interface revisited, *Sci. Rep.*, 2019, **9**, 2259.
2 M. Thoma and H. Möhwald, Monolayers of dipalmitoylphosphatidylcholine at the oil-water interface, *Colloids Surf., A*, 1995, **95**, 193–200, DOI: **10.1016/0927-7757(94)03021-Q**.
3 P. Gao, X. Xing, Y. Li, T. Ngai and F. Jin, Charging and discharging of single colloidal particles at oil/water interfaces, *Sci. Rep.*, 2014, **4**, 4778.
4 R. Aveyard, J. H. Clint, D. Nees and V. N. Paunov, Compression and Structure of Monolayers of Charged Latex Particles at Air/Water and Octane/Water Interfaces, *Langmuir*, 2000, **16**, 1969–1979, DOI: **10.1021/la990887g**.
5 J. J. Benkoski, R. L. Jones, J. F. Douglas and A. Karim, Photocurable Oil/Water Interfaces as a Universal Platform for 2-D Self-Assembly, *Langmuir*, 2007, **23**(7), 3530–3537.
6 J. Zhai, A. J. Mile, L. K. Pattende, T.-H. Lee, M. A. Augustin, B. A. Wallace, M.-I. Aguilar and T. J. Wooster, Changes in β-Lactoglobulin Conformation at the Oil/Water Interface of Emulsions Studied by Synchrotron Radiation Circular Dichroism Spectroscopy, *Biomacromolecules*, 2010, **11**(8), 2136–2142.
7 A. R. Zimmer, A. Oliboni, S. L. C. Viscardi, R. M. Teixeira, M. F. Ferrão and F. M. Bento, Biodiesel blend (B10) treated with a multifunctional additive (biocide) under simulated stored conditions: a field and lab scale monitoring, *Biofuel Res. J.*, 2017, **4**(2), 627–636.
8 L. Hu, M. Chen, X. Fang and L. Wu, Oil–water interfacial self-assembly: a novel strategy for nanofilm and nanodevice fabrication, *Chem. Soc. Rev.*, 2012, **41**, 1350–1362.
9 B. Belaissaoui, J. Claveria-Baro, A. Lorenzo-Hernando, D. A. Zaidiza, E. Chabanon, C. Castel, S. Rode, D. Roizard and E. Favre, Potentialities of a dense skin hollow fiber membrane contactor for biogas purification by pressurized water absorption, *J. Membr. Sci.*, 2016, **513**, 236–249.
10 M. M. Fernandez, R. M. Wagterveld, S. Ahualli, F. Liu, A. V. Delgado and H. V. M. Hamelers, Polyelectrolyte-versus membrane-coated electrodes for energy production by capmix salinity exchange methods, *J. Power Sources*, 2016, **302**, 387–393.
11 B. S. Lalia, V. Kochkodan, R. Hashaikeh and N. Hilal, A review on membrane fabrication: structure, properties and performance relationship, *Desalination*, 2013, **326**, 77–95.
12 E. Kang, J. Ryoo, G. S. Jeong, Y. Y. Choi, S. M. Jeong, J. Ju, S. Chung, S. Takayama and S. H. Lee, Large-scale, ultrapliable, and free-standing nanomembranes, *Adv. Mater.*, 2013, **25**, 2167–2173.
13 A. L. Thangawng, R. S. Ruoff, M. A. Swartz and M. R. Glucksberg, An ultra-thin PDMS membrane as a bio/micro-nano interface: Fabrication and characterization, *Biomed. Microdevices*, 2007, **9**, 587–595.
14 F. Peng, Z. Jiang, C. Hu, Y. Wang, H. Xu and J. Liu, Removing benzene from aqueous solution using CMS-filled PDMS pervaporation membranes, *Sep. Purif. Technol.*, 2006, **48**, 229–234.
15 A. El Haitami, E. H. G. Backus and S. Cantin, Synthesis at the Air-Water Interface of a Two-Dimensional Semi-Interpenetrating Network Based on Poly(dimethylsiloxane)

and Cellulose Acetate Butyrate, *Langmuir*, 2014, **30**, 11919–11927.

16 C. Kim, M. C. Gurau, P. S. Cremer and H. Yu, Chain conformation of poly(dimethyl siloxane) at the air/water interface by sum frequency generation, *Langmuir*, 2008, **24**, 10155–10160.

17 D. Lin, S. Y. Jin, F. Zhang, C. Wang, Y. Q. Wang, C. Zhou and G. J. Cheng, 3D stereolithography printing of graphene oxide reinforced complex architectures, *Nanotechnology*, 2015, **26**(43), 434003.

18 T. Femmer, A. J. C. Kuehne, J. Torres-Rendon, A. Walther and M. Wessling, Print your membrane: rapid prototyping of complex 3D-PDMS membranes via a sacrificial resist, *J. Membr. Sci.*, 2015, **478**, 12–18.

19 T. Femmer, A. J. C. Kuehne and M. Wessling, Print your own membrane: direct rapid prototyping of polydimethylsiloxane, *Lab Chip*, 2014, **14**, 2610–2613.

20 S. Badalov, Y. Oren and C. J. Arnusch, Ink-jet printing assisted fabrication of patterned thin film composite membranes, *J. Membr. Sci.*, 2015, **493**, 508–514.

21 J. J. Martin, B. E. Fiore and R. M. Erb, *Nat. Commun.*, 2015, **6**, 8641.

22 S. Park, M. R. Abdul Hamid and H.-K. Jeong, Highly Propylene-Selective MixedMatrix Membranes by in Situ Metal Organic FrameworkFormation Using a Polymer-Modification Strategy, *ACS Appl. Mater. Interfaces*, 2019, **11**(29), 25949–25957.

23 P. P. Wang, J. Ma, F. M. Shi, Y. X. Ma, Z. H. Wang and X. Y. Zhao, Behaviors and effects of differing dimensional nanomaterials in water filtration membranes through the classical phase inversion process: a review, *Ind. Eng. Chem. Res.*, 2013, **52**, 10355–10363.

24 L. Y. Ng, A. W. Mohammad, C. P. Leo and N. Hilal, Polymeric membranes incorporated with metal/metal oxide nanoparticles: a comprehensive review, *Desalination*, 2013, **308**, 15–33.

25 N. Peng, N. Widjojo, P. Sukitpaneenit, M. M. Teoh, G. G. Lipscomb, T. S. Chung and J. Y. Lai, Evolution of polymeric hollow fibers as sustainable technologies: Past, present, and future, *Prog. Polym. Sci.*, 2012, **37**, 1401–1424.

26 L. Cheng, A. R. Shaikh, Li-F. Fang, S. Jeon, C.-J. Liu, L. Zhang, H.-C. Wu, D.-M. Wang and H. Matsuyama, Fouling-Resistant and Self-Cleaning Aliphatic Polyketone Membrane for Sustainable Oil–Water Emulsion Separation, *ACS Appl. Mater. Interfaces*, 2018, **10**(51), 44880–44889.

27 A review on models and simulations of membrane formation *via* phase inversion processes, Y. Tang, Y. Lin, D. M. Ford, X. Qian, M. R. Cervellere, P. C. Millett and X. Wang, *J. Membr. Sci.*, 2021, **640**, 119810, DOI: **10.1016/j.memsci.2021.119810**.

28 G. R. Guillen, Y. Pan, M. Li and E. M. V. Hoek, Preparation and Characterization of Membranes Formed by Nonsolvent Induced Phase Separation: A Review, *Ind. Eng. Chem. Res.*, 2011, **50**, 3798–3817, DOI: **10.1021/ie101928r**.

29 S. Coppola, G. Nasti, V. Vespini, L. Mecozzi, R. Castaldo, G. Gentile, M. Ventre, P. A. Netti and P. Ferraro, Quick liquid packaging: Encasing water silhouettes by three-dimensional polymer membranes, *Sci. Adv.*, 2019, **5**, eaat5189.

30 J.-P. Cohen Addad and R. Pedro-Born, Phase-inversion membranes. Characterisation of patterns of skin holes, *Macromol. Chem. Phys.*, 1995, **196**, 3615–3621, DOI: **10.1002/macp.1995.021961115**.

31 G. R. Guillen, Y. Pan, M. Li and E. M. V. Hoek, Preparation and Characterization of Membranes Formed by Nonsolvent Induced Phase Separation: A Review, *Ind. Eng. Chem. Res.*, 2011, **50**, 3798–3817, DOI: **10.1021/ie101928r**.

32 F. Merola *et al.*, Recent advancements and perspective about digital holography: A super-tool in biomedical and bioengineering fields, *Advancement of Optical Methods & Digital Image Correlation in Experimental Mechanics*, Springer, Cham, 2019, vol. 3, pp. 235–241.

33 B. Mandracchia, *et al.*, Quantitative imaging of the complexity in liquid bubbles' evolution reveals the dynamics of film retraction, *Light: Sci. Appl.*, 2019, **8**(1), 20.

34 Z. Wang, L. Miccio, S. Coppola, V. Bianco, P. Memmolo, V. Tkachenko, V. Ferraro, E. Di Maio, P. Luca Maffettone and P. Ferraro, Digital holography as metrology tool at micro-nanoscale for soft matter, *Light: Adv. Manuf.*, 2022, **3**, 10.